ELSEVIER

Thermochimica Acta 254 (1995) 337-345

thermochimica
acta

Application of thermal analysis techniques to a sample of Red Mud — a by-product of the Bayer process — for magnetic separation [☆]

L. Piga [a], F. Pochetti [b,*], L. Stoppa [b]

[a] *CNR Mineral Processing Institute, Via Bolognola 7, Rome, Italy*
[b] *Department of Chemical Engineering, "La Sapienza" University, Via Eudossiana, 18 00184 Rome, Italy*

Received 4 January 1994; accepted 11 July 1994

Abstract

In a sample of Red Mud, a by-product of the Bayer process, the reduction of ferric oxides to elemental iron and magnetite, performed prior to subjecting the sample to magnetic separation, was followed by thermogravimetric and differential thermal analysis (TGA/DTA) in an oxidizing atmosphere. The relative quantities of metallic iron and magnetite in the reduced sample can be estimated from the oxidation thermogram; in the case of the magnetic fraction, obtained via magnetic separation of the reduced sample, the absolute quantity of metallic iron and magnetite can be estimated from the relative thermogram.

Keywords: Coupled technique; Haematite; Magnetite; Oxidation; Red Mud

1. Introduction

The Red Mud (RM) residues formed during the extraction of alumina from bauxite by the Bayer process contain titanium, iron and aluminium compounds that could provide an interesting source of raw materials for relevant processing industries. At the present time RM is disposed of in Italy by controlled on-shore

---

* Corresponding author.

[☆] Dedicated by the co-authors to Professor Pochetti on the occasion of his sixtieth birthday.

SSDI 0040-6031(94)01988-6

discharge; in France and Japan the waste is discharged into the sea. Both solutions could cause serious environmental problems and involve an expense that reflects on the production cost of the alumina. Many technologies have been proposed for recovery of the metal contained in the RM [1–5]. One of the most promising concerns processes which, in the initial stage, involve magnetic separation with the production of two fractions. The iron-rich fraction could possibly be used by the steel industry, while the other, rich in aluminium and titanium, could be further processed for the recovery of these two metals. Prior to magnetic separation, the ferric oxides (maghemite and haematite) present in the RM have to be transformed into highly paramagnetic oxides (magnetite) [6–8]. The scope of the work reported here was to use thermogravimetric analysis and differential thermal analysis (TGA/DTA) to keep a quantitative check on this transformation to metallic iron and magnetite. Numerous studies have been conducted over the years to determine which mechanism is involved in the oxidation of magnetite. These studies have generally been performed in an oxygen atmosphere on samples of very pure natural and man-made magnetite. It is commonly accepted that oxidation of magnetite to α-Fe_2O_3 (haematite) occurs in two stages in the 275–375°C and 500–650°C temperature ranges [9]. Depending on the specific surface of the sample, in the second stage either the magnetite that is still not reduced is oxidized or the γ-$Fe_2O_3 \rightarrow \alpha$-$Fe_2O_3$ transition occurs [10]. According to Lepp [11], the formation of γ-Fe_2O_3 in the first stage is favoured by a high specific surface, and Egger and Feitknecht [10] hold that this is due to the rapid diffusion of oxygen into the crystal lattice without significant alteration of the structure: in fact, the crystal structure of magnetite is more similar to maghemite (γ-Fe_2O_3) than to haematite (α-Fe_2O_3). Colombo et al. [12] believe that the specific surface factor is important only in surface oxidation, while the degree of the crystalline order plays a decisive role as regards the nature of the products deriving from the first stage of oxidation.

2. Methods of calculation

The weight loss or weight gain during the reduction of a sample of pure Fe_2O_3 to metallic iron or magnetite and the subsequent inverse reaction of oxidation of the same sample can be ascertained by simple stoichiometric calculations

$$Fe_2O_3 + 3H_2 \rightarrow 2Fe + 3H_2O \qquad \Delta P/\% = -30.0 \tag{1}$$

$$2Fe + \tfrac{3}{2}O_2 \rightarrow Fe_2O_3 \qquad \Delta P/\% = 42.9 \tag{2}$$

$$3Fe_2O_3 + H_2 \rightarrow 2Fe_3O_4 + H_2O \qquad \Delta P/\% = -3.33 \tag{3}$$

$$2Fe_3O_4 + \tfrac{1}{2}O_2 \rightarrow 3Fe_2O_3 \qquad \Delta P/\% = 3.45 \tag{4}$$

In the case of a sample containing other metal oxides and assuming that the ferric oxides can be reduced simultaneously to metallic iron and magnetite, the variables that influence the above weight variations are both the Fe_2O_3 content of the mixture and the fraction, indicated by [Fe], of Fe_2O_3 in the sample reduced to metallic iron.

Consequently $[1-\text{Fe}]$ indicates the Fe_2O_3 fraction of the sample reduced to magnetite, so the weight gain due to oxidation can be calculated by

$$\Delta P/\% = \%\text{Fe}_2\text{O}_3 \times \left[\frac{[\text{Fe}] \times 0.30}{1 - 0.30 \times (\%\text{Fe}_2\text{O}_3/100) \times [\text{Fe}]} + \frac{[1-\text{Fe}] \times 0.03335}{1 - 0.0333 \times (\%\text{Fe}_2\text{O}_3/100) \times [1-\text{Fe}]}\right] \quad (5)$$

For instance, with a sample of Red Mud containing 31.61% Fe_2O_3, as in the case of the work described here, the expected weight loss would be 9.48% according to Eq. (1) when there is complete reduction to metallic iron ($[\text{Fe}] = 1$) and the subsequent increase due to oxidation would be 10.48% according to Eq. (5). In the event of complete reduction to magnetite the loss during reduction would be 1.05% according to Eq. (3) and the increase during the subsequent oxidation would be 1.07% according to Eq. (5). In the reverse procedure, if the weight gain during the oxidation of a sample containing a known quantity of Fe_2O_3 is ascertained by TGA, then the fraction of iron in the sample that is reduced to metallic iron [Fe] and magnetite $[1-\text{Fe}]$ can be calculated.

3. Experimental

3.1. Characterization

The sample of Red Mud utilized came from the Portovesme aluminium plant (Sardinia). The grain-size distribution and chemical analyses of the calcined sample (Table 1) indicate that this is very fine material (80% <3 μm) containing a fair amount of TiO_2 (12.1%) and Al_2O_3 (25.3%). The XRD spectrum of the calcined sample (Fig. 1) reveals the presence of haematite only.

Table 1

Grain size distribution of raw Red Mud and chemical analysis of a calcined (800°C) sample of Red Mud

Size/μm	Proportion/%	Oxide	%
>6.0	2.27	Fe_2O_3	31.6
6.0–3.1	17.76	Al_2O_3	25.3
3.1–1.8	23.49	SiO_2	13.2
1.8–0.9	33.43	TiO_2	12.1
<0.9	23.05	CaO	7.7
Total	100.00	Na_2O	7.7
		Other	2.4
		Total	100.0

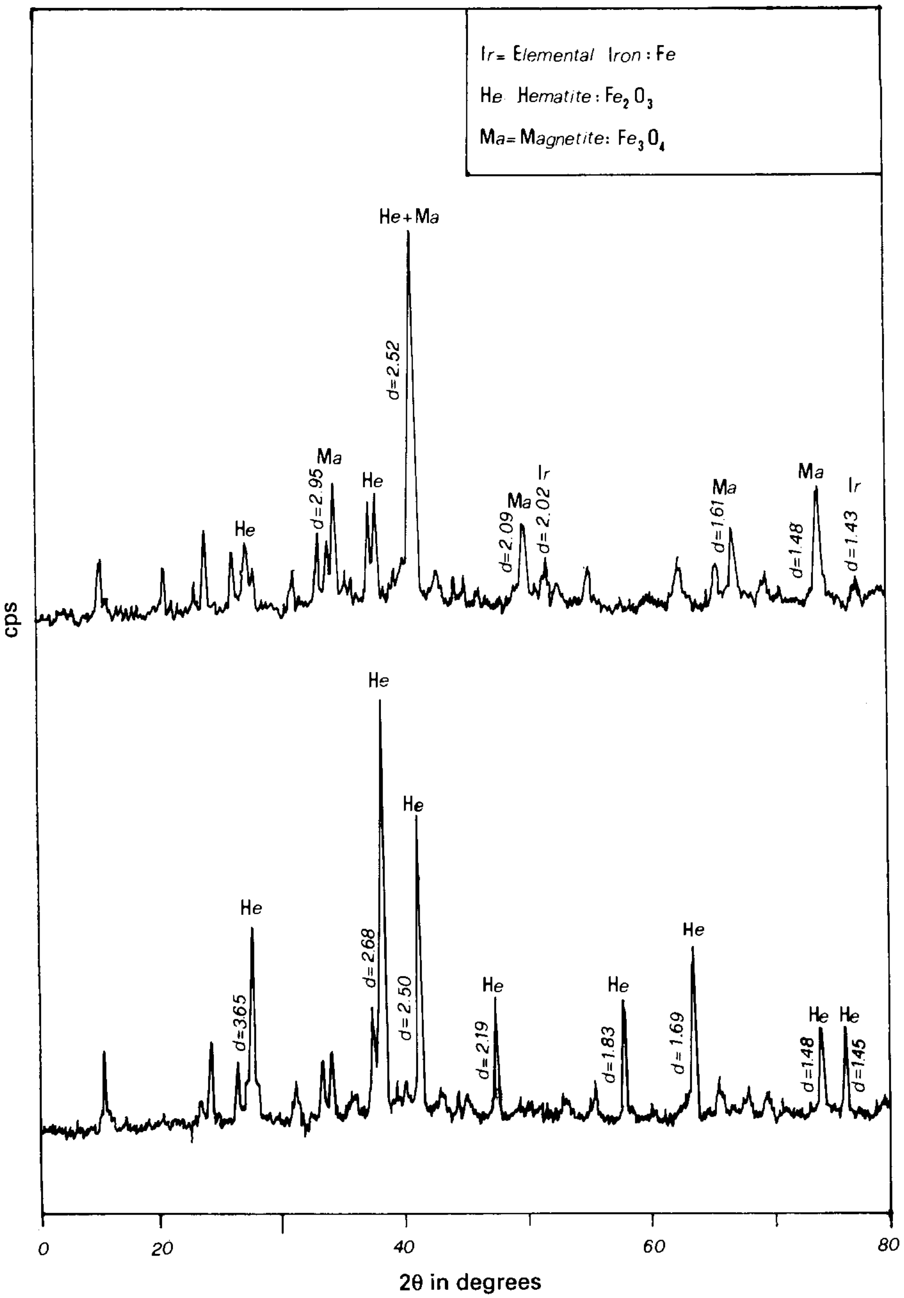

Fig. 1. XRD spectra (Cu Kα radiation) of a calcined (below) and reduced (above) sample of Red Mud derived from alumina production.

3.2. Reduction of sample

Ten grams of RM calcined at 800°C were placed on a porous disc fixed in the centre of a quartz tube 50 cm high and 4 cm in diameter enclosed in a vertical tubular furnace. A stream of reducing gas (200 ml min^{-1}) consisting of three parts H_2 and seven parts N_2 was introduced via the lower end of the reactor so as to simulate a fluidized-bed system. After 3 h of operation at 500°C the reactor was cooled to room temperature in an inert atmosphere. When selecting the reduction temperature, account was taken of the fact that, according to the Fe/O phase diagram [13], undesirable non-magnetic wustite (FeO) is formed at temperatures greater than 570°C. The absence of wustite is confirmed by the XRD spectrum of the reduced sample given in Fig. 1. In fact, only metallic iron, magnetite and unreduced haematite are present. The intensity of the principal haematite peaks is lower than that of the peaks in the calcined sample, the exceptions being the ones at $2\theta = 41.6$ and 74.6° which are common to haematite and magnetite, thus confirming the presence of the latter phase in the reduced sample.

In preliminary tests the RM samples were reduced by means of various gases, including CH_4, CO and H_2. It was found that H_2 permitted the most precise reading of the thermograms. In fact, the use of CO results in the formation of carbon black at 500°C as in the reaction $2CO = C + CO_2$, which causes interference in the subsequent analysis of the samples by TGA/DTA.

3.3. Oxidation of reduced sample and magnetic fraction

3.3.1. Thermal appartus

The tests were performed using a Model 1500 Stanton Redcroft thermobalance with a sensitivity of 1 μg, temperature range 20–1500°C and heating rate 0.1–50°C min^{-1}. The furnace winding is made of rhodium–platinum and the thermocouple is located under the rhodium–platinum crucible containing the sample. The heating rate in the tests was 10°C min^{-1} in a stream of reducing gas or air. The weight of the sample was about 80 mg in each test and the scale factor (SF) was 0.04 mg mm^{-1}.

3.3.2. Oxidation of the reduced sample

As can be seen from the thermogram in Fig. 2, the weight gain of the sample during oxidation (2.2%) is intermediate between the theoretical values expected in the case of the presence of metallic iron only and magnetite only, which indicates that both phases are present. Eq. (5) yields $[\mathrm{Fe}] = 0.133$ and so $[1 - \mathrm{Fe}] = 0.867$ which is equivalent to 3.00% metallic iron and 27.1% Fe_3O_4, assuming that all the ferric oxides present in the calcined sample participate in the reduction to elemental iron and magnetite. The ratio of Fe_3O_4 to Fe is thus 9.04.

3.3.3. Oxidation of magnetic fraction

The sample reduced to iron and magnetite was subjected to low-intensity magnetic separation (0.1 Tesla) to obtain an iron-enriched magnetic fraction. The

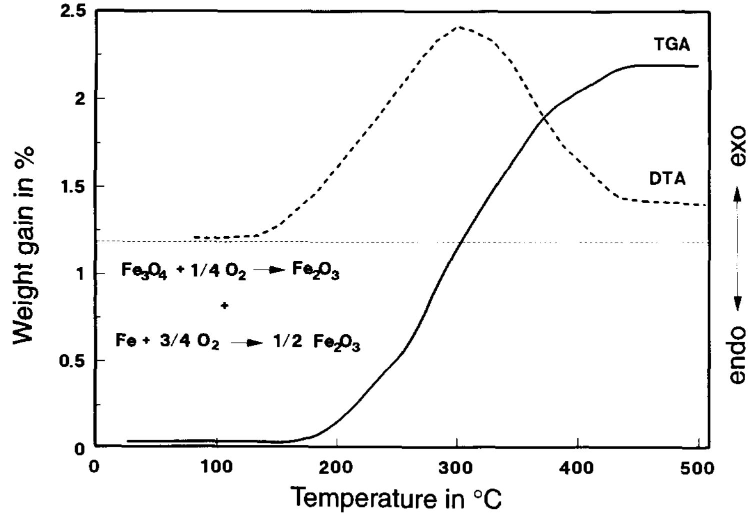

Fig. 2. Thermogram relative to oxidation of a reduced sample of Red Mud; 10°C min^{-1} in a stream of air.

average weight gain obtained from oxidation of the magnetic fraction, one of whose thermograms is illustrated in Fig. 3, is 4.41%. The variability of the analytical results was calculated by submitting three portions of the same sample to TGA/DTA; the standard deviation was quite low: 0.08%. There are two reasons for the

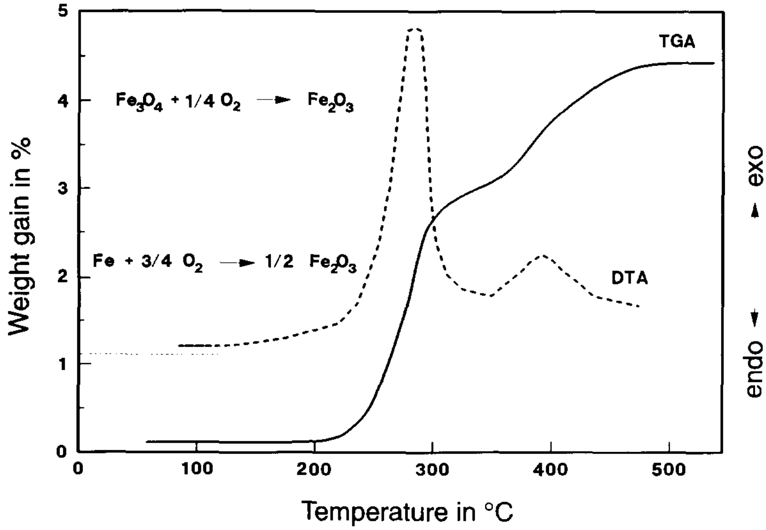

Fig. 3. Thermogram relative to oxidation of the magnetic fraction obtained after magnetic separation of a reduced sample of Red Mud; 10°C min^{-1} in a stream of air.

greater weight gain compared with that (2.20%) obtained from oxidation of the sample reduced prior to magnetic separation. Firstly there is the obvious fact that the magnetic fraction contains more iron and magnetite than does the reduced sample. And secondly, the metallic-iron/magnetite ratio of the magnetic fraction is higher than that of the feed. In fact, as the magnetic susceptibility of metallic iron is far greater than that of magnetite, when free grains of iron and magnetite are treated the former are attracted preferentially into the magnetic fraction.

It is apparent from the thermogram that there are two weight-gain steps separated by an inflexion, the first within the 210–330°C temperature range and the second between 330°C and 480°C. If it is assumed that the first step, corresponding to a weight gain of 2.95%, is attributable to the oxidation of metallic iron as per Eq. (2), it can be calculated that the magnetic fraction contains 6.88% metallic iron. Similarly, if the second step, corresponding to a weight gain of 1.46%, is attributable to oxidation of the magnetite as per Eq. (4), then it can be calculated that there is 42.6% magnetite in the magnetic fraction. The ratio between the values found is 6.19, which is lower than that for the reduced sample prior to magnetic separation (9.04). This confirms that iron has a greater tendency to be attracted into the magnetic fraction than has magnetite. If the final product of oxidation is expressed as Fe_2O_3, the content of metallic iron and magnetite present in the magnetic fraction amounts to 53.9% (the sum of the two phases). However, as chemical analysis of the sample indicates that the Fe_2O_3 content of the magnetic fraction is 61.3%, the difference between the two values (7.4%) represents haematite that has remained unaltered during reduction of the calcined sample.

4. Simulation

A simulation has been performed to verify the hypothesis that the two steps in the thermogram during oxidation of the magnetic fraction are attributable respectively to the oxidation of metallic iron and magnetite. Let us consider the equation

$$42.86\frac{a}{100}+3.45\frac{b}{100}=4.41 \tag{6}$$

which correlates experimental weight gain of the thermogram due to simultaneous oxidation of the metallic iron (a) and the magnetite (b) present in the magnetic fraction, as in Eqs. (2) and (4). Because the values of a and b are not known, it is assumed that their sum S lies between 30.11 and 100. The first figure represents the sum of the metallic iron and magnetite values in the reduced sample prior to magnetic separation, and it would be the same in the magnetic fraction if magnetic separation produced no enrichment. The value 100 represents the metallic iron and magnetite content of the magnetic fraction in the ideal case of perfect enrichment, namely if the magnetic fraction consisted solely of metallic iron and magnetite. Now if b in Eq. (6) is substituted by $(S-a)$, an equation is obtained involving only

Table 2
Results of simulation of Eq. (6) (see text)

S	Fe (a)	Fe_3O_4 (b)	Fe_2O_3	Fe_3O_4/Fe
30.0	8.58	21.4	34.4	2.50
30.5	8.54	22.0	34.9	2.57
31.0	8.50	22.5	35.4	2.65
31.5	8.45	23.0	35.9	2.73
32.0	8.41	23.6	36.4	2.81
32.5	8.37	24.1	36.9	2.88
⋮	⋮	⋮	⋮	⋮
48.5	6.99	41.5	52.9	5.94
49.0	6.95	42.1	53.4	6.05
49.5	**6.90**	**42.6**	**53.9**	**6.17**
50.0	6.86	43.1	54.4	6.29
50.5	6.82	43.7	54.9	6.41
51.0	6.77	44.2	55.4	6.53
⋮	⋮	⋮	⋮	⋮
57.9	6.17	51.7	62.3	8.37
58.0	6.18	51.8	62.4	8.40
58.1	6.16	51.9	62.5	8.43
58.2	6.15	52.0	62.6	8.46
58.3	6.14	52.2	62.7	8.48
58.4	6.13	52.3	62.8	8.52
⋮	⋮	⋮	⋮	⋮
59.5	6.04	53.5	63.9	8.85
59.6	6.03	53.6	64.0	8.88
59.7	6.02	53.7	64.1	8.91
59.8	6.01	53.8	64.2	8.94
59.9	6.00	53.9	64.3	8.97
60.0	6.00	54.0	64.4	9.00

S and a. Then by varying S between the extreme values 30.11 and 100, values of a and hence b are obtained compatible with the weight gain recorded by the thermogram. Table 2 gives the results of the simulation relating to a number of S values (column 1) lying between 30 and 60. Columns 2 and 3 indicate the pairs of metallic iron and magnetite values, while column 4 gives the sums of the column 2 and 3 values expressed as Fe_2O_3. Column 5 sets forth the ratio of the magnetite and metallic iron values. Examination of the table to find the metallic-iron/magnetite ratio closest to that derived from the thermogram considering the individual weight gains reveals that for $S = 49.5$ the pair of metallic iron and magnetite values that satisfies Eq. (6) is 6.90 and 42.6% respectively. These values are virtually the same as those found previously from the individual weight gains, thus confirming the hypothesis advanced regarding the source of the two curves.

5. Conclusions

By analysing the thermogravimetric curve obtained from oxidation of a reduced sample of Red Mud, a by-product of the Bayer process, it is possible to ascertain the relative quantities of iron and magnetite present. If the reduced sample is then submitted to magnetic separation and the magnetic fraction is subjected to oxidation, it is found that there are two weight gains at different temperatures (the thermogram has two steps). By ascribing the two weight gains to the oxidation of the iron and the magnetite, respectively, it is possible to estimate the absolute quantity of iron and magnetite present in the sample. Stoichiometric calculations made on the basis of the total weight gain resulting from oxidation of the magnetic fractions confirm that the two steps derive from oxidation of the iron and the magnetite respectively. This approach provides a rapid, precise method for determining the magnetite and metallic iron content of the feed and products obtained when reduced Red Mud is subjected to magnetic separation.

Acknowledgement

The authors thank Mrs S. Severi for the part she has played in drafting this paper.

References

[1] P.J. Cresswell and D.J. Milne, Australian Patent 88102, 1981.

[2] W.H. Andrews, West German Patent 3720444-A1, 1981.

[3] V.G. Logomerac, Rud. Metal. Zb., 4 (1976) 313.

[4] E. Guccione, Eng. Min. J., 9 (1971) 136.

[5] O.C. Fursman, J.E. Mauser, M.O. Butler and W.A. Stickney, Report Invest. 7454, US Bureau of Mines, 1970, pp. 1–31.

[6] M. Braithwaite, British Patent 2078211-A, 1982.

[7] D. Buttinelli, L. Chacon, L. Piga, F. Pochetti, J. Sorrentino and L. Stoppa, In Proc. Int. Cong., Energy, Environment and Technological Innovation, held in Rome, Italy, September 1992, Vol. 2 pp. 291–296.

[8] L. Sadler and C. Venkataraman, Int. J. Miner. Process., 31 (1991) 233.

[9] M.A. Gheith, Am. J. Sci., 250 (1952) 677.

[10] K. Egger and W. Feitknecht, Helv. Chim. Acta, 45 (1962) 2042.

[11] H. Lepp, Econ. Geol., 57 (1962) 260.

[12] U. Colombo, G. Fagherazzi, F. Gazzarrini, G. Lanzavecchia and G. Sironi, Chim. Ind. (Milan), 46 (1964) 357.

[13] L.S. Darken and R.W. Gurry, in M.K. Reser (Ed.), Phase Diagrams for Ceramists, 4th edn., The American Ceramic Society Inc., 1979, p. 37.